



# Comparative study on a deactivation kinetic model based on fractional conversion of solid in fluid/solid heterogeneous processes

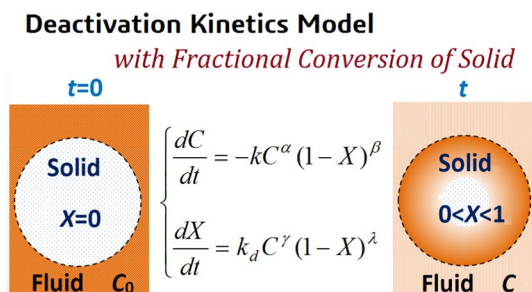
Kye-Ryong Sin<sup>1</sup> · Yong-Son Hong<sup>2</sup> · Ju-Gyong Kim<sup>1</sup> · Wi-Ryong Choe<sup>2</sup> · Kwang-Song Kim<sup>2</sup> · Yong-Man Jang<sup>1</sup>

Received: 13 March 2024 / Accepted: 22 April 2024 / Published online: 7 June 2024  
© Akadémiai Kiadó, Budapest, Hungary 2024

## Abstract

In this work, the definition of deactivation kinetic model (DKM) has been given under some assumptions and its features were illustrated through comparison with prior kinetic models such as DM (deactivation model), Langmuir rate equation, pseudo kinetic model and unreacted SCM (shrinking core model). DKM is based on fractional conversion of solid and concentration of fluid phase, which is one of the different kinetic models for the heterogeneous processes. DKM has no thermodynamic equilibrium quantities such as adsorption amount ( $q_e$ ) unlike the previous pseudo-order models. Therefore, DKM can offer more accurate kinetic parameters than other models. Main equations of DKM can be solved by using Matlab functions such as “ODE” and “lsqnonlin”. This DKM is a semi-empirical and apparent kinetic model for fluid/solid heterogeneous processes and its kinetic equations can be used not only in heterogeneous reactions, but also in adsorption processes.

## Graphical abstract



**Keywords** Kinetic modeling · Heterogeneous reaction · Adsorption · Deactivation kinetic model

Extended author information available on the last page of the article

**Table 1** Kinetic models on the heterogeneous processes

Model	Kinetic equations
SCM [6]	$t = \frac{\rho_B R_p}{3bM_B k_g C_{Ag}} X + \frac{\rho_B R_p^2}{6bM_B D_e C_{Ag}} [1 - 3(1 - X)^{2/3} + 2(1 - X)] + \frac{\rho_B R_p}{bM_B k_s C_{Ag}} [1 - (1 - X)^{1/3}]$
GM [7]	$\frac{dr}{dt} = -\frac{k}{\rho_m} \left\{ C_A \left( 1 + \frac{D'_A}{D'_C K_E} \right) - \frac{1}{K_E} \left[ C_{A0} + \left( \frac{D'_A}{D'_C} - 1 \right) C_R \right] \right\}$
RPM [12, 13]	$X = 1 - \left( 1 - \frac{k_s C^n t}{R_0} \right) \exp \left[ -\frac{k_s C^n S_0 t}{1 - \epsilon_0} \left( 1 + \frac{\pi L_0 k_s C^n t}{S_0} \right) \right]$
DM [21–24]	$-\frac{ds}{dt} = k_d s - \frac{da}{dt} = k_d C_A^n a^m,$
DKM [32–37]	$\frac{dX}{dt} = k_d C_A^n (1 - X)^\lambda$

## Introduction

Heterogeneous systems are included in many chemical processes such as gas purification, wastewater treatment, heterogeneous catalysis, adsorption and extractive metallurgy, where chemical reaction or adsorption occurs at the interface between the phases in heterogeneous processes. The rate of a surface reaction might depend on various factors such as pressure, temperature and catalyst.

The rate in heterogeneous reactions can be expressed as Eq. 1 [1].

$$r = \frac{1}{\nu_j} \frac{d\sigma_j}{dt} \quad (1)$$

here  $r$  is the rate of reaction,  $\nu_j$  is the stoichiometric number of species ( $j$ ),  $\sigma_j = n_j/A$ ,  $n_j$  is the amount of substance (number of moles) of species ( $j$ ) and  $A$  is the surface area. The rates of heterogeneous reactions were expressed in moles per square meter per second ( $\text{mol m}^{-2} \text{s}^{-1}$ ).

But Eq. 1 has not been used widely in practice, because the  $\nu_j$ ,  $n_j$  and  $A$  are indeterminable exactly in many real systems. Therefore, tens of different kinetic models for heterogeneous reactions were proposed. Development in kinetics of non-catalytic gas/solid reactions has been summarized in the previous literatures [2, 3]. Table 1 shows some typical kinetic models on the heterogeneous processes.

The unreacted SCM (shrinking core model) [4, 5, 62] assumed that the reaction occurs at the interface between the reacted outer surface and the unreacted interior core and the diffusion through the solid product layer obeys Fick's law with a constant diffusion coefficient. Diffusion into solid reactant is much slower than reaction rate, which is suitable mainly for solid sorbents with low porosity, but not for solid sorbents with mesoporous structure [6].

The grain model (GM) [7] on porous solid reactant has been proposed and used. Wen and Ishida [8], Hartman and Coughlin [9] employed GM and used the porosity as a function of conversion. Ramachandran and Smith [10] proposed the single-pore model and took into account the change of pore structure. Focusing

on the change of grain size, Georgakis et al. [11] presented the changing grain size model: the grain radius changes during the reaction as a function of  $Z$  which is the ratio between the molar volumes of the solid product and the solid reactant.

Bhatia and Perlmutter [12, 13] presented the random pore model (RPM) for fluid–solid reaction that was suitable for unsupported solid [14, 15]. They used a pore structure parameter ( $\psi$ ) to characterize solid reactivity and correlated  $\psi$  with  $m$ , which was used as the grain shape factor [3] or the order of reaction [16] in prior models. Some studies have been done on kinetic model of hot coal gas desulfurization [17–19].

The deactivation model (DM) [20] was applied successfully [21] in adsorption of volatile organic compounds on granular activated carbon. Yasyerli et al. [22–24] applied DM to predict the  $H_2S$  breakthrough curves over a variety of sorbents, which agreed well with the experimental results. According to this model, the effects of the textural variation (pore structure, active surface area and formation of production per unit area) of the solid sorbent were expressed in deactivation rate. The deactivation rate of the solid sorbent was expressed as Eq. 2.

$$-\frac{da}{dt} = k_{d0} C_A a \quad (2)$$

here  $a$  is the activity of the solid sorbent [22],  $k_{d0}$  is the deactivation rate constant and  $C_A$  is the concentration of gas. The reaction order was assumed to be 1 for gas and sorbent and all factors such as pore structure and active surface area of the sorbent were included in the activity term ( $a$ ). Dahlan et al. [25] and Ficicilar et al. [26] reported similarly that the deactivation rate of solid reactant (sorbent) was independent of the concentration of gaseous reactant, which means that the deactivation rate was zero order with respect to gaseous reactant in DM. The empirical deactivation laws in DM for a variety of catalysts were summarized in Ref. [27]. Tang and Yang [28] proposed a “deactivation model” as Eq. 3, which is a parabola equation and can be applied in gas adsorption systems with gas concentration from low level to relatively high one by considering the effect of catalyst deactivation.

$$r = kKC - AC^2 \quad (3)$$

here  $r$  is the reaction rate,  $k$  is the rate constant,  $K$  is the equilibrium constant,  $C$  is the inlet concentration of gas.  $A$  is defined as deactivation coefficient ( $A > 0$ ) which indicates the effect of photocatalyst deactivation on the reaction rate.

Some researchers investigated on a couple of “deactivation kinetic model” (DKM) [29–31], but their physical meanings were different one another. Martin et al. [29] proposed a DKM based on the postulates of Langmuir–Hinshelwood and used it for the catalyst deactivation by coke in heterogeneous polymerizations. DKMs from Emadoddin et al. [30] and Ko [31] were the same as the previous DM (Eq. 2) in essence.

Hong et al. presented a modified DKM (See Eq. 4 in Sect. “Methodology”) and applied it on some heterogeneous processes [32–37], which showed that this DKM can be used not only in heterogeneous reaction but also in adsorption.

In this work, to make clear the physical background of our modified DKM based on fractional conversion of solid and support its wider application, we formulated it under a few of reasonable assumptions and its validity was checked up through kinetic analysis of different experimental and simulated data in comparison with prior kinetic models. The advantages and disadvantages in the application of the DKM were verified.

## Methodology

The definition of DKM has been given under some assumption and the methodology of calculation was explained.

### Definition of DKM and the kinetic equations using it in batch and continuous system

One of the difficult problems in the kinetic analysis of fluid/solid heterogeneous processes is how to express the characteristics of solid surface where reaction or adsorption can occur. In order to solve this problem, we used the fractional conversion of the solid phase as the major scale to formulate a new DKM. To this end, the following assumptions were presented:

- (i) Fractional conversion ( $X$ ) of solid phase is defined as the ratio (dimensionless) of the used portion to the initial one of solid, which is 0 at fresh solid ( $t=0$ ) and 1 at maximum saturation (or complete usage of solid for reaction or adsorption) state.
- (ii) Variation rate of solid phase is expressed as a function of  $X$  and  $C$  (concentration of fluid phase), which is the deactivation rate of solid. The change of fluid concentration with time is also expressed as a function of  $X$  and  $c$ .
- (iii) Reaction orders of all species in the heterogeneous process are not assumed, but are calculated from the measured kinetic experimental data and rate equation.

The change of fractional conversion in solid phase with time is expressed as shown in Eq. 4:

$$\frac{dX}{dt} = k_d C^\gamma (1 - X)^\lambda \quad (4)$$

here  $k_d$  is the deactivation rate constant of solid,  $C$  is the concentration of fluid ( $\text{mol dm}^{-3}$ ) and  $\gamma$ ,  $\lambda$  are the reaction orders of fluid and solid.  $(1 - X)$  is the portion of solid where the reaction or the adsorption can proceed further at given time ( $t$ ).

This DKM based on the fractional conversion of solid is an apparent kinetic model on the solid reactant with a semi-empirical rate equation (Eq. 4). It can be called “Hong’s DKM” in distinction from other DKMs [29–31] and hereafter it is called DKM for simplicity.

In batch system, the rate equation from DKM on the reaction between a fluid and a solid phase or single component adsorption is Eq. 5.

$$\begin{cases} \frac{dC}{dt} = -kC^\alpha(1-X)^\beta \\ \frac{dX}{dt} = k_d C^\gamma(1-X)^\lambda \end{cases} \quad (5)$$

here  $k$  is the apparent rate constant of fluid and  $\alpha, \beta, \gamma, \lambda$  are the reaction orders.

The results calculated from various kinetic parameters (reaction orders and rate constants) were shown in Fig. 1, where the default values of all other parameters were fixed as 1 when the effect of one kinetic parameter was investigated.  $C/C_0$  (dimensionless concentration) and  $X$  curves have different shapes according to the change of kinetic parameters.

Kinetic parameters such as reaction order and rate constant can be evaluated by using experiment data and calculated curves. To be concrete, the kinetic parameters were calculated using the nonlinear least-squares fitting (“lsqnonlin” function of MATLAB was used.) of the fluid concentration calculated by solving Eq. 5 to the corresponding experimental data.

The rate equation on the reaction between two fluid species and a solid phase or binary adsorption is the extension of Eq. 5, which can be derived as Eq. 6.

$$\begin{cases} \frac{dC_1}{dt} = -k_1 C_1^{\alpha_1} (1-X)^{\beta_1} \\ \frac{dC_2}{dt} = -k_2 C_2^{\alpha_2} (1-X)^{\beta_2} \\ \frac{dX}{dt} = k_d (C_1 + C_2)^\gamma (1-X)^\lambda \end{cases} \quad (6)$$

here  $k_1, k_2$  are the rate constants of fluid species 1 and 2,  $C_1, C_2$  are the corresponding concentrations,  $\alpha_1, \beta_1, \alpha_2, \beta_2$  are the reaction orders.

Equations 5 and 6 are the kinetic equations in batch system from DKM, which can be called “Hong’s equation”.

This DKM is applicable in continuous system (ex. the fixed-bed reactor). If the plug flow of fluid and the pseudo-steady state are assumed, the time derivative of fluid concentration ( $C$ ) is much smaller than the spatial derivative of  $C$  on most non-catalytic gas–solid reactions [6, 41, 42]. Equation 7 was derived from the mass balance equation and DKM as following [32]:

$$\begin{cases} \frac{\partial C}{\partial z} = -\frac{k_a}{u} C^\alpha (1-X)^\beta \\ \frac{\partial X}{\partial t} = k_d \cdot C^\gamma (1-X)^\lambda \end{cases} \quad (7)$$

here  $k_a$  is the rate constants of apparent chemical reaction,  $u$  is the inlet flow rate of gas,  $z$  is the distance from the reactor entrance to given point.

The breakthrough curves were calculated on various kinetic parameters (Fig. 2).

As shown in Fig. 2, the breakthrough curves calculated on various kinetic parameters have different forms and the following results can be obtained from them:

- (i) Reaction orders affect the profile of breakthrough curve and the influence of  $(1-X)$ 's order is more extreme than that of  $C$ 's order.

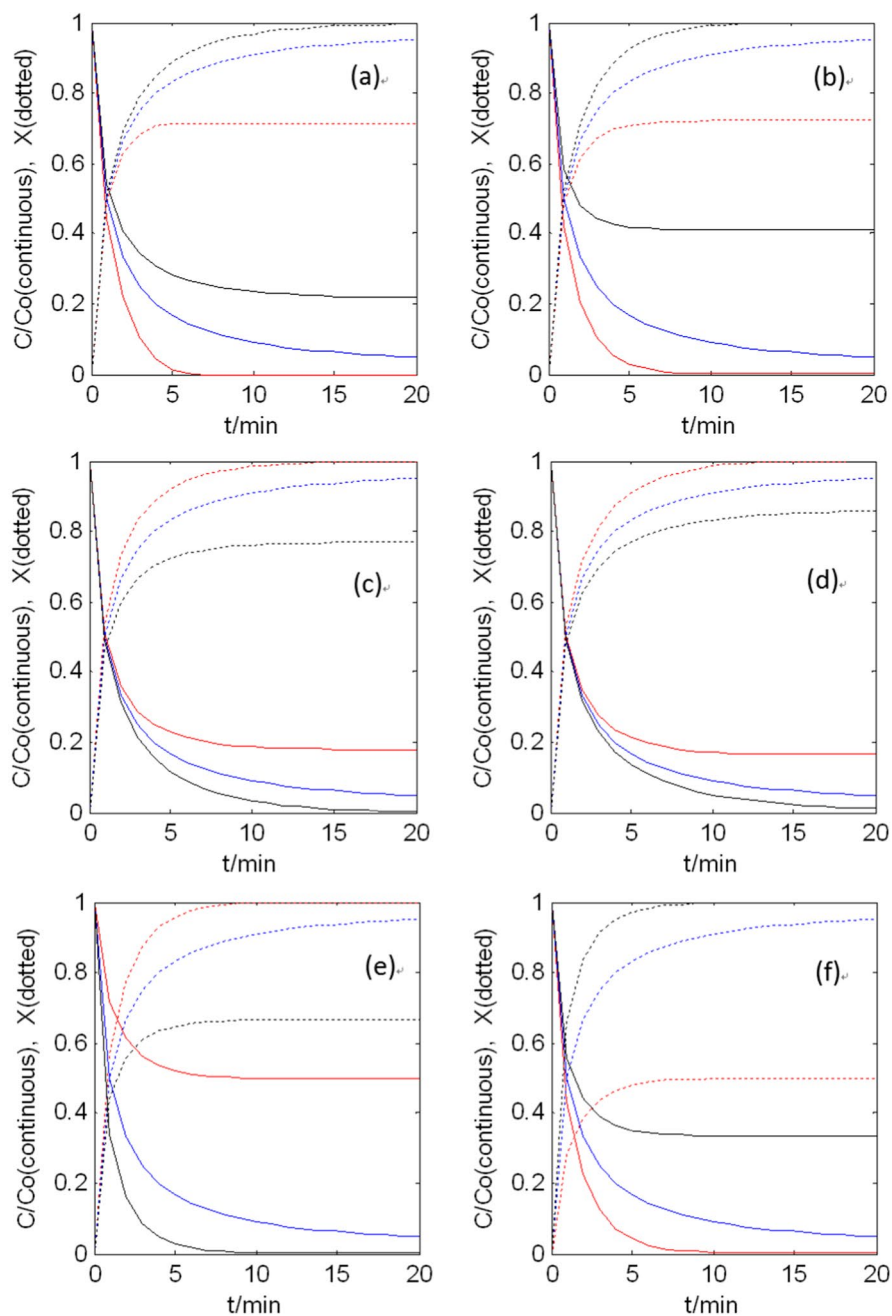


**Fig. 1**  $C/C_0$  and  $X$  calculated on various kinetic parameters: **a**  $\alpha=0.6$  (red), 1.0 (blue), 1.4 (black), **b**  $\beta=0.4$  (red), 1.0 (blue), 1.7 (black), **c**  $\gamma=0.8$  (red), 1.0 (blue), 1.2 (black), **d**  $\lambda=0.7$  (red), 1.0 (blue), 1.3 (black), **e**  $k_a=0.7$  (red), 1.0 (blue), 1.3 (black), **f**  $k_d=0.6$  (red), 1.0 (blue), 1.4 (black). (Color figure online)

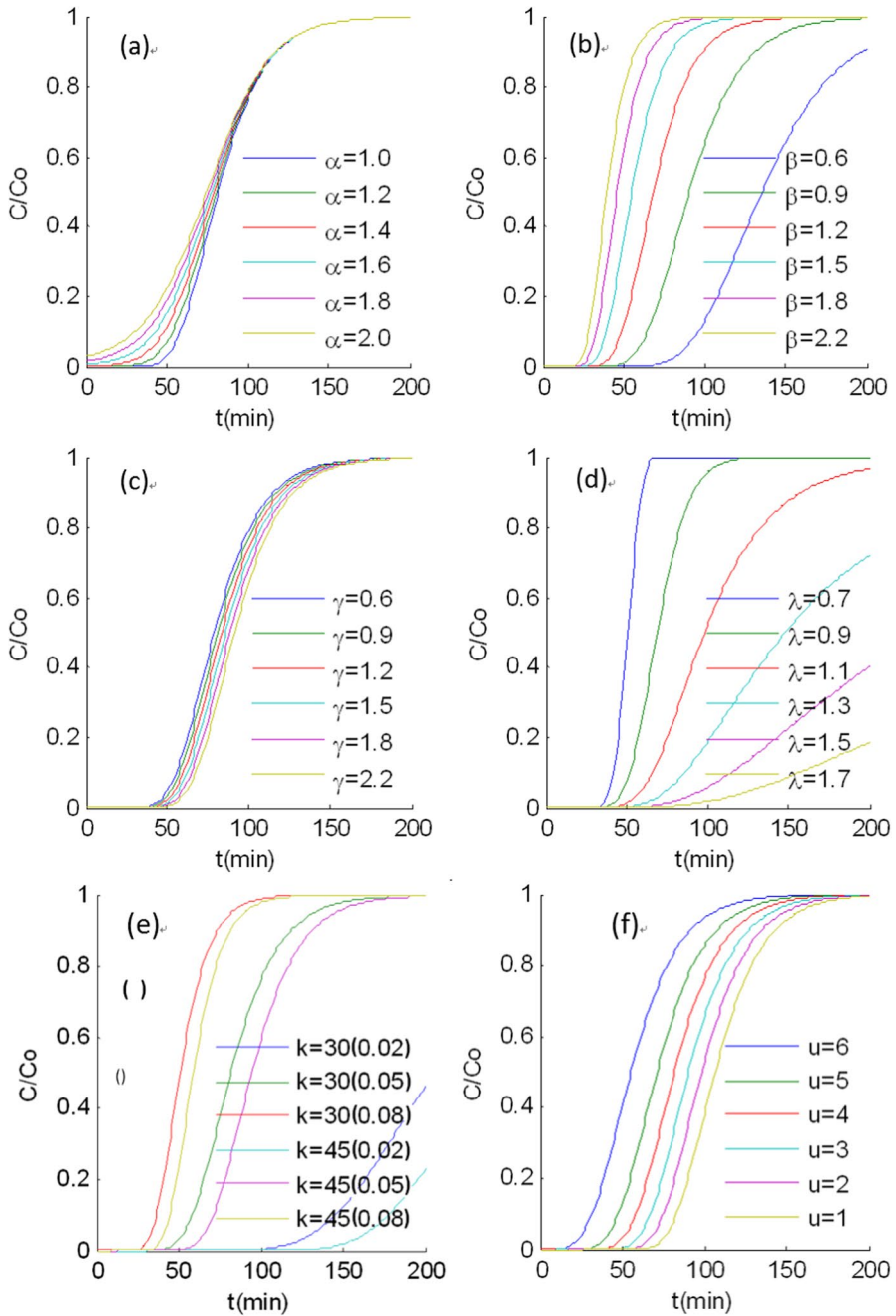


**Fig. 2** The breakthrough curves calculated on various kinetic parameters: **a**  $\alpha$ , **b**  $\beta$ , **c**, **d**  $\lambda$ , **e**  $k$ , **f**  $u$ ;  $k = k_a$ ,  $k = k_d$

- (ii) Rate constants affect the profile of breakthrough curve and the breakthrough time. The larger  $k_a$  is, the longer breakthrough time is. The larger  $k_d$  is, the steeper gradient of breakthrough curve is and the shorter breakthrough time is.
- (iii) Flow rate of gas has no effect on the profile of breakthrough curve, but affects the breakthrough time.

### Calculation on the kinetic equations as an example

Equation 5 is a set of simultaneous ordinary differential equations, in which both fluid and solid are considered explicitly and can be solved with ODE function (functions for solving ordinary differential equations) in MATLAB.

Both partial differential equations (Eq. 7) are solved simultaneously using forward finite differential method [43] by employing initial ( $x=0$  for all position  $z$  at  $t=0$ ) and boundary ( $C=C_0$  for all time  $t$  at  $z=0$ ) conditions.

The kinetic parameters (rate constants and orders of reaction) were calculated using the nonlinear least-squares fitting of the concentration obtained by solving Eqs. 5 or 7 to the corresponding experimental data. The object function of least-squares fitting for reaction rate constants and orders was calculated as the following Eq. 8:

$$\min f(k_a, k_d) = \sum_i^{n_i} (C_{cal} - C_{exp})^2 \quad (8)$$

here  $k$  is the apparent rate constants,  $n_i$  is the number of experimental point,  $C_{cal}$  is the concentration simulated by solving Eqs. 5 or 7 and  $C_{exp}$  is concentration from experiments.

The input data required for the nonlinear optimization is only the non-dimensionalized concentration ( $C/C_0$ ) of the adsorbates with time and  $X$  (fractional conversion in solid phase with time) is automatically evaluated in the calculation process. As a result, the kinetic parameters and  $X$  are obtained simultaneously.

The kinetics of cadmium (II) ion adsorption by three soil samples was evaluated in batch experiments. All experiments were carried out in 250 mL glass flasks by adding 1 g soil to 100 mL cadmium ion solution (100 mg/L). The 250 mL glass flasks were shaken in different time periods at a constant speed of 100 rpm in a constant temperature shaker at 25 °C. All experiments were performed at pH  $4 \pm 0.5$ , adjusted by the drop wise addition of 0.1 mol/L HCl. All samples were allowed to rest for 10 min after the experiment and the concentration of metal ions in the filtrate was measured by atomic absorption spectroscopy.

The concentration of adsorbates (Fig. 3a) calculated by Eq. 5 shows that the experimental data agree well with the curves calculated by Eq. 5. The  $X$  (fractional conversion of adsorbents) calculated by Eq. 5 was shown in Fig. 3b.

If all reaction orders were equal to 1, the correlation coefficient became smaller than 0.8 and some calculated adsorption rate constants became smaller than 0. When the reaction order was evaluated  $\alpha = 1.5$ , the correlation coefficient became larger than 0.99, the experimental data agree well with the calculated curves.



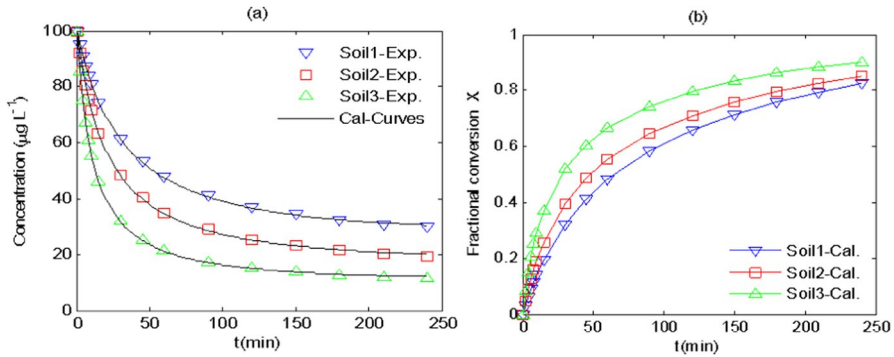


**Fig. 3** C-curves and X calculated on various rate constants (reaction orders:  $\alpha = \beta = \gamma = 1, \lambda = 1.5$ )

The rate constants (Table 2) calculated by Eqs. 5 and 8 show that the calculated rate constants can quantitatively be compared on both adsorbate and adsorbents unlike PSO model.

According to Eq. 5, the effects of the textural variation (pore structure, active surface area and so on per unit area) of the adsorbent and the formation of adsorbed layer were popularly expressed in terms of  $k_d$  (deactivation rate constant, i.e. the change of fractional conversion with time in solid phase).

### Results and discussion

The features of the DKM were illustrated through comparison with prior kinetic models such as DM, Langmuir rate equation, pseudo kinetic model and unreacted SCM in the batch or the fixed-bed reactor.

#### Comparison of DKM with DM and Langmuir rate equation

The features of DKM were compared with prior kinetic models (DM and Langmuir rate equation).

DKM has no regard the detailed characteristic parameters of solid phase in such a microscopic way as SCM, GM and RPM, but in a macroscopic way. According to DKM, the rate of variation (pore structure, active surface area and

**Table 2** Rate constants calculated by Eqs. 5 and 8

Soil sample	$k_d/\text{min}^{-1}$	$k_d/L \mu\text{g}^{-1} \text{min}^{-1}$	$R^2$
Soil 1	0.0242	0.0169	0.9999
Soil 2	0.0409	0.0250	0.9999
Soil 3	0.0836	0.0471	0.9999

the formation of product layer per unit area) of solid was expressed in term of deactivation rate like that in DM.

DKM and DM [20–28] seem to be almost the same, but there is distinction between them. In DM, the reaction order of deactivation was assumed to be first-order with respect to solid surface and to be first (or zero)-order for concentration of fluid phase. But in DKM, all the reaction orders were not assumed, but calculated. In some previous works using DM [24–28],  $a$  (activity of the solid due to textural change) was used in the initial kinetic equation, but was not referred in the kinetic analysis on experimental data, because  $a$  had completely petered out during derivation of the final kinetic equation. That is,  $a$  can be seen to be a qualitative term on solid reactant, which was introduced in order to establish the kinetic model (DM), but  $X$  in DKM is quantitative value to be estimated in the kinetic analysis on solid reactant.

Langmuir rate equations based on  $\theta$  (fractional coverage) have been well-known. Among Langmuir rate Equations, Eq. 9 was used for single adsorption, Eq. 10 was used in competitive adsorption [38–40] and Eq. 11 is the Langmuir–Hinshelwood model used in the heterogeneous processes [66, 67].

$$\frac{d\theta}{dt} = k_A C(1 - \theta) - k_D \theta \quad (9)$$

$$\begin{cases} \frac{d\theta_1}{dt} = k_{A1} C_1 [1 - (\theta_1 + \theta_2)] - k_{D1} \theta_1 \\ \frac{d\theta_2}{dt} = k_{A2} C_2 [1 - (\theta_1 + \theta_2)] - k_{D2} \theta_2 \end{cases} \quad (10)$$

$$-\frac{dC}{dt} = kf(C) = k \frac{KC}{1 + KC} \quad (11)$$

here  $k_A$  is the adsorption rate constant and  $k_D$  is the desorption rate constant,  $C_1$ ,  $C_2$  are the concentration of fluid species 1 and 2,  $C$  is the reactants concentration;  $t$  is the reaction time,  $k$  represents the rate constant,  $f(C)$  is a function of the concentration of species and  $K$  is the adsorption equilibrium constant.

There are clear distinctions between Hong's equations (Eqs. 5 and 6) and Langmuir rate equations (Eqs. 9, 10 and 11) as follows:

- (i) Langmuir rate equations are the concrete expression for adsorption and desorption processes. But, Hong's equations are the overall one, assuming the equilibrium states of adsorption and desorption at every moment.
- (ii)  $\theta$  in Langmuir rate equations is the concept based on monolayer adsorption (chemical adsorption), but  $X$  in Hong's equations is used without such a limit. Therefore, it can be used not only for monolayer adsorption, but also for multilayer adsorption including physical adsorption, and becomes to be a more comprehensive concept than  $\theta$ .
- (iii) Adsorbate concentration is a constant in Langmuir rate equations (Eqs. 9, 10), but the change of adsorbate concentration and fractional conversion of adsor-

bent with time are simultaneously reflected in Hong's equations for adsorption system.

- (iv) On a competitive adsorption, the fractional coverages of adsorbent occupied by each adsorbate are estimated in Langmuir rate equations, but the overall fractional conversion of adsorbent is estimated in Hong's equation (Eq. 6).
- (v) The Langmuir–Hinshelwood model (Eq. 11) involved the values of the adsorption equilibrium constants ( $K$ ). If the reaction temperature changes, the  $K$  would change, too. This brings about lead to the bad result in the kinetic study, i. e. the temperature dependence of the rate constant can't be calculated accurately. But Hong's equation (Eq. 6) hasn't any thermodynamic equilibrium quantity.

Dozens of the experimental data from the previous papers were kinetically reevaluated by using Hong's equations [34–37], where reaction orders and activation energies were newly obtained.

### Comparison of DKM with pseudo kinetic models in adsorption system

Investigation on adsorption kinetic models has been continued to obtain more correct models to fit the experimental data, which resulted in many kinetic models. Therefore, users of those models had difficulty to choose a specific model for their own experimental data. In the past decades, the correlation coefficients between the experimental data and the simulated ones by a couple of available kinetic models were calculated to find out the best fitting model. This has been the common and traditional way for starting a research on adsorption kinetics. Experimental data obtained from different systems and experimental conditions can need different models for optimal fitting with the simulated values. But it is almost impossible to compare the kinetic parameters obtained from different models.

The pseudo kinetic models have been used widely [63–65], but it involved an adsorption amount ( $q_e$ ), which is not a kinetic quantity, but a thermodynamic equilibrium quantity. Therefore the rate constants calculated by the pseudo kinetic models can't be compared with each other accurately.

In order to examine whether Hong's equations can be generally applied in kinetic analysis on different adsorption systems, the rate constants and reaction orders were calculated by Hong's equations on the basis of previous experimental data simulated by twelve pseudo kinetic models [44–53]. As shown in Table 3, all correlation coefficients ( $R^2$ ) between the simulated data by pseudo kinetic models and the calculated ones by Hong's equations were 1.0000 or 0.9999. It shows that Hong's equations can offer universal interpretation on the experimental data, which had to be treated by different pseudo kinetic models.

In common, there are two components (an adsorbate and an adsorbent) at least in single adsorption system. Both adsorbate and adsorbent must be considered in the rate equation so as to estimate the kinetic characteristics of the system. But the pseudo kinetic models considered only the adsorbent. Hong's equations can solve this problem.

**Table 3** Pseudo kinetic models and parameters calculated by Hong’s equations

No.	Pseudo kinetic models		Parameters calculated by Hong’s equations							
	Name	Equation	Parameters	$\alpha$	$\beta$	$\gamma$	$\lambda$	$k_a$	$k_d$	$R^2$
1.	Pseudo-first-order (PFO) [44]	$\frac{dq}{dt} = k_1(q_e - q)$	-	Ref. [37]						1.0000
2.	Pseudo-second-order (PSO) [45]	$\frac{dq}{dt} = k_2(q_e - q)^2$	-	Ref. [37]						1.0000
3.	Pseudo-n-order (PnO) [46]	$\frac{dq}{dt} = k_n(q_e - q)^n$	-	Ref. [37]						1.0000
4.	Mixed-order (MOE) [47]	$\frac{dq}{dt} = \frac{k_1}{1-f_2}(1-F)(1-f_2F)$	$k_n = 0.1$ $f_2 = 0.5$	2	1	2	1	0.0601 ± 0.0010	0.2043 ± 0.0010	1.0000
5.	Modified PFO (MPFO-1) [48]	$\frac{dq}{dt} = k_1(q_e/q)(q_e - q)$	$k_1 = 0.1$	2	2	2	1	0.9664 ± 0.0173	0.7705 ± 0.0034	1.0000
6.	Modified PFO (MPFO-2) [49]	$\frac{dq}{dt} = k_1(q_e^2/q^2)(q_e - q)$	$k_1 = 0.1$	2	2	2	1	4.3667 ± 0.1997	2.7418 ± 0.0234	1.0000
7.	Modified PSO (MPSO-1) [49]	$\frac{dq}{dt} = k_2(q_e/q)(q_e - q)^2$	$k_2 = 0.1$	2	2	2	1.5	0.7311 ± 0.0149	0.6280 ± 0.0081	0.9999
8.	Modified PSO (MPSO-2) [49]	$\frac{dq}{dt} = k_2(q_e^2/q^2)(q_e - q)^2$	$k_2 = 0.1$	2	2	2	1.5	2.1781 ± 0.0973	1.6584 ± 0.0895	0.9999
9.	Modified PnO (MPnO) [49]	$\frac{dq}{dt} = k_n(q_e^{n-1}/q^{n-1})(q_e - q^n)$	$k_n = 0.1$ $n = 1.25$	2	2	2	1	0.0802 ± 0.0011	0.1962 ± 0.0096	1.0000
			$k_n = 0.1$ $n = 1.50$	2	2	2	1	0.2325 ± 0.0153	0.3430 ± 0.0089	1.0000
			$k_n = 0.1$ $n = 1.75$	2	2	2	1	0.4794 ± 0.0128	0.5523 ± 0.0296	1.0000
			$k_n = 0.1$ $n = 2.0$	2	2	2	1	0.8521 ± 0.0601	0.8411 ± 0.0099	1.0000
10.	Fractal-like PFO (FPFO) [50, 51]	$\frac{dq}{dt} = k_1 t^\alpha (q_e - q)$	$k_n = 0.1$ $\alpha = 0.3$	10	10	10	2.5	2.5355 ± 0.0781	0.6785 ± 0.0177	1.0000
			$k_n = 0.1$ $\alpha = 0.7$	10	10	10	1.5	0.2548 ± 0.0259	0.1942 ± 0.0118	1.0000
11.	Fractal-like PSO (FPSO) [50, 51]	$\frac{dq}{dt} = k_2 t^\alpha (q_e - q)^2$	$k_n = 0.1$ $\alpha = 0.3$	20	20	20	9.0	3.5432 ± 0.0580	1.3889 ± 0.0186	1.0000
			$k_n = 0.1$ $\alpha = 0.7$	20	20	20	3.1	0.4643 ± 0.0789	0.3138 ± 0.0339	1.0000

**Table 3** (continued)

No.	Pseudo kinetic models	Parameters calculated by Hong's equations									
		Name	Equation	Parameters	$\alpha$	$\beta$	$\gamma$	$\lambda$	$k_a$	$k_d$	$R^2$
12.	Fractal-like MOE(FMOE) [50, 51]	$\frac{dF}{dt^n} = \frac{k_1 F}{1-f_2} (1-F)(1-f_2 F)$ $k_n = 0.1$	$\alpha = 0.2$	11	11	11	6.8	$16.2015 \pm 1.1486$	$6.3789 \pm 0.3937$	1.0000	
			$f_2 = 0.5$								
			$\alpha = 0.5$	10	10	10	2.8	$2.8322 \pm 0.3077$	$1.3280 \pm 0.1109$	1.0000	
			$f_2 = 0.5$								
			$\alpha = 0.8$	8	8	8	1.5	$0.3784 \pm 0.0926$	$0.3767 \pm 0.0494$	0.9999	
			$f_2 = 0.5$								
13.	Fractal-like Exp (FEXM) [51]	$\frac{dF}{dt^n} = k' [\exp(1-F) - 1]$	$k_n = 0.1$	20	20	20	9.0	$3.8474 \pm 0.1738$	$2.2771 \pm 0.0997$	0.9999	
			$\alpha = 0.3$								
			$k_n = 0.1$	5	5	5	1.5	$0.3157 \pm 0.0256$	$0.2694 \pm 0.0123$	1.0000	
			$\alpha = 0.7$								
14.	Exponential kinetic model (ExM) [52]	$\frac{dF}{dt} = kF[\exp(1-F) - 1]$	$k_n = 0.1$	1	1	1	1	$0.0693 \pm 0.0032$	$0.1661 \pm 0.0154$	1.0000	
15.	Hyperbolic tangent model (HTM) [53]	$\frac{dF}{dt} = q_0 k(1 - \tanh^2 kt)$	$k_n = 0.1$	1	0.7	1	0.7	$0.0073 \pm 0.0004$	$0.1162 \pm 0.0127$	0.9999	

Hong's equation is a kinetic equation without any thermodynamic equilibrium quantity. Activation energy can't be evaluated by many of previous adsorption kinetic models such as the pseudo-order models. Because pseudo-models involve the adsorption amount  $q_e$ , which is not a kinetic quantity in strict meaning, but a thermodynamic equilibrium quantity. When Arrhenius equation is used to calculate activation energy, the rate constants must be constant at given temperature. However, not only the rate constant, but also the adsorbed amount  $q_e$  change with temperature in the pseudo-models, so the temperature dependence of the rate constant can't be calculated accurately. There are some difficulties in calculation of the kinetic parameters, but the ordinary differential equations and optimization solutions are not so difficult if the calculation tools such as Matlab are used. Utilization of DKM in interpretation of adsorption kinetics is only on the beginning stage and how the parameters of adsorption kinetic equation are changed in chemical adsorption and physical one are still the remained problems to be studied further.

In order to compare DKM with PSO, U (VI) adsorption on several adsorbents [54–59] were kinetically reevaluated using Eq. 5, by which the reaction orders were newly calculated and the rate constants were quantitatively calculated on both adsorbate and adsorbent (Table 4).

As shown in Table 4, the reaction order of (1-X) on each adsorbent was newly estimated as 1–1.5 and the rate constants on both adsorbate and adsorbent were calculated. In comparison with PSO, the following results can be obtained:

- (i) From PSO analysis, U (VI) adsorption mechanisms on various adsorbents seem to be the same [54–59]. But DKM showed that the concrete mechanisms for different adsorbents might be different because their reaction orders ( $\lambda$ ) calculated by Hong's equations were not the same.

**Table 4** Kinetic parameters for U (VI) adsorption on various adsorbents

Adsorbent*	PSO			Hong's equation, $\alpha=\beta=\gamma=1$			
	$k_2$ ( $\text{g mg}^{-1} \text{min}^{-1}$ )	$q_e$ ( $\text{mg g}^{-1}$ )	$R^2$	$\lambda$	$k_a$ ( $\text{min}^{-1}$ )	$k_d$ ( $\text{L mg}^{-1} \text{min}^{-1}$ )	$R^2$
ISCB [54]	0.00159	162.85	0.9952	1.0	$0.1872 \pm 0.0098$	$0.2127 \pm 0.0034$	1.0000
AHR [55]	0.0046	62.11	0.9900	1.2	$0.3067 \pm 0.0126$	$0.3839 \pm 0.0274$	1.0000
Carbon-LSs + CTAB [56]	0.00004533	134.1	0.9976	1.2	$0.0047 \pm 0.0003$	$0.0081 \pm 0.0004$	1.0000
Polypyrrole [57]	0.0609	42.016	0.9997	1.3	$2.5969 \pm 0.0783$	$4.4452 \pm 0.1089$	1.0000
AALW [58]	0.0004	95.51	0.9980	1.4	$0.0234 \pm 0.0011$	$0.0699 \pm 0.0029$	1.0000
POP-EDVP [59]	0.00388	102.45	0.9999	1.5	$0.2112 \pm 0.0126$	$1.0210 \pm 0.0999$	1.0000

\*ISCB=Immobilized Saccharomyces Cerevisiae Beads, AHR=Cation exchange resin Amberjet 1200 H, Carbon-LSs + CTAB= Mesoporous carbon using sodium lignosulfonate (LSs) as a raw material and cetyltrimethylammonium bromide (CTAB) as a template agent, AALW= Alkali-activated leather waste, POP-EDVP= Novel nanoporous organic polymer adsorbent P

- (ii)  $k_2$  determined by PSO for different adsorbents can't be compared with each other because their  $q_e$  were not the same. But  $k_a$  and  $k_d$  by Hong's equations can be compared between different adsorbents when their reaction orders are the same. For example, two adsorbents (AHR and Carbon-LSs + CTAB) have the same reaction orders ( $\lambda = 1$  0.2). Therefore, their  $k_a$  and  $k_d$  can be compared with each other, quantitatively.

### Comparison of DKM with SCM in the fixed-bed reactor (continuous system)

The fixed-bed reactor is one of the continuous reactors. In this case, the kinetic model needs a set of simultaneous partial differential equations unlike above examples. That is, the kinetic model on the fixed-bed reactor should be expressed as a function of time ( $t$ ) and position ( $z$ ).

Lee and Koon [6] proposed the modified SCM for the reaction between sulfur dioxide and coal fly ash/CaO/CaSO<sub>4</sub> sorbent in the fixed-bed reactor. Their model (Eq. 12) was used in predicting the whole duration of the desulfurization reaction, yielding an average deviation between the simulated and experimental data to be less than 5%.

$$\left\{ \begin{array}{l} \frac{\partial C}{\partial z} = -\frac{LA_s S_e \beta (C_{SO})^f (C_{NO})^g C(1-bX)^h}{nV_R} \exp\left(-\frac{E_a}{RT}\right) \\ \frac{\partial X}{\partial t} = \alpha e^{aT} (C_{SO})^c (RH)^d (1-bX)^e \beta C_{SO}^f \exp\left(-\frac{E_a}{RT}\right) \frac{3bC}{\rho_p r} (1-X)^{2/3} \end{array} \right. \quad (12)$$

here  $C$  is the concentration of SO<sub>2</sub> at given time,  $C_{SO}$  and  $C_{NO}$  are the initial concentration of SO<sub>2</sub> and NO,  $X$  is the sorbent utilization,  $L$  is the fixed-bed reactor length,  $A_s$  is the transversal bed section,  $S_e$  is the specific surface area of sorbent,  $n$  is the initial molar flow rate of SO<sub>2</sub>,  $V_R$  is the volume of reaction bed,  $\rho_p$  is the sorbent density,  $r$  is the radius of unreacted core, RH is the relative humidity. The estimated values of  $\alpha$ ,  $\beta$ ,  $E_a$ ,  $a$ ,  $b$ ,  $c$ ,  $d$ ,  $e$ ,  $f$ ,  $g$  and  $h$  were 1309.5, 0.121 m/s, 16,200 J·mol<sup>-1</sup>, -0.02 K<sup>-1</sup>, 12, 0.2, -3, 5, 0.1, 0.75 and 4.

On the other hand, Hong et al. [32, 33] applied DKM in kinetic analysis of H<sub>2</sub>S removal over mesoporous La-Fe mixed oxide/MCM-41 [60], Cu-Mn mixed oxide/SBA-15 [61] and La-Mn mixed oxide/KIT-6 [61] sorbents during hot coal gas desulfurization in the fixed-bed reactor. By using Eq. 13 [32] as the estimated kinetic equation of H<sub>2</sub>S removal over mesoporous La-Fe mixed oxide/MCM-41, the average deviation between calculated H<sub>2</sub>S concentration and experimental data became lower than 1%.

$$\left\{ \begin{array}{l} \frac{\partial C}{\partial z} = -\frac{849800L}{u} C(1-X)^{2/3} \exp\left(-\frac{3860}{T}\right) \\ \frac{\partial X}{\partial t} = 0.5056 \cdot C^{3/2} (1-X) \exp\left(-\frac{1818.4}{T}\right) \end{array} \right. \quad (13)$$

By comparing Eq. 13 with Eq. 12, the following results were obtained:

- (i) In theoretical view, Eq. 12 is more concrete than Eq. 13 because it includes many factors which can affect the reaction rate. But Eq. 13 has the deactivation rate constant of solid to embrace these factors.
- (ii) In view of practical utilization, Eq. 13 is more convenient than Eq. 12 because there is no vague values which is changed with time or difficult to measure unlike Eq. 12 with such a value (radius of unreacted core).

Therefore, Eq. 13 from DKM seems to be an omnibus and useful kinetic model.

## Conclusion

The DKM formulated based on the fractional conversion of solid phase is one of heterogeneous kinetic models, which is a semi-empirical, apparent kinetic and generalized model. The kinetic equations from DKM for batch system and continuous system can be used not only in heterogeneous reactions, but also in adsorption processes. The relationship between the kinetic parameters of DKM and composition or surface structure of solid phase and mechanisms of heterogeneous reaction needs more investigation in future.

**Author contributions** Conceptualization: WRC; Methodology: YSH; Formal analysis and investigation: JGK, KSK; Writing—original draft preparation: YMJ; Writing—review and editing: KRS.

**Funding** This research did not receive any specific grant from funding agencies in the public, commercial, or not-for-profit sectors.

**Data availability** The data sets supporting the results presented in the study have been generated using the MATLAB code.

## Declarations

**Conflict of interest** The authors declare that they have no conflict of interest.

## References

1. Atkins P, Paula J (2006) Physical chemistry. W.H. Freeman and Company, New York
2. Ramachandran PA, Doraiswamy LK (1982) Modeling of noncatalytic gas-solid reactions. *AIChE J* 28:881–900
3. Szekey J, Evans JW, Sohn HY (1976) Gas–solid reactions. Academic Press, New York
4. Do DD (1982) On the validity of the shrinking core model in noncatalytic gas solid reaction. *Chem Eng Sci* 37:1477–1481
5. Erk HF, Dudukovic MP (1984) Self-inhibited rate in gas-solid noncatalytic reaction. The shrinking core model. *Ind Eng Chem Res* 23:49–54
6. Lee KT, Koon OW (2009) Modified shrinking unreacted-core model for the reaction between sulfur dioxide and coal fly ash/Cao/CaSO<sub>4</sub> sorbent. *Chem Eng J* 146:57–62
7. Szekey J, Evans JW (1971) A structural model for gas-solid reactions with a moving boundary II: the effect of grain size, porosity and temperature on the reaction of porous pellets. *Chem Eng Sci* 26:1901–1913



8. Wen CY, Ishida M (1973) Reaction rate of sulphur dioxide with particles containing calcium oxide. *Environ Sci Technol* 7:703–708
9. Hartman M, Coughlin RW (1976) Reaction of sulphur dioxide with limestone and the grain model. *AIChE J* 22:490–498
10. Ramachandran PA, Smith JM (1977) Transport rates by moment analysis of dynamic data. *AIChE J* 23:353–361
11. Georgakis C, Chang CW, Szekely J (1979) A changing grain size model for gas–solid reactions. *Chem Eng Sci* 34:1072–1075
12. Bhatia SK, Perlmutter DD (1980) A random pore model for fluidsolid reactions: I. Isothermal kinetic control. *AIChE J* 26:379–386
13. Bhatia SK, Perlmutter DD (1981) A random pore model for fluidsolid reactions: II. Diffusion and transport effects. *AIChE J* 27:247–254
14. Ebrahim HA (2010) Application of random-pore model to SO<sub>2</sub> capture by lime. *Ind Eng Chem Res* 49:117–122
15. Singer SL, Ghoniem AF (2011) An adaptive random pore model for multimodal pore structure evolution with application to char gasification. *Energy Fuels* 25:1423–1437
16. Krishnan SV, Sotirchos SV (1993) A variable diffusivity shrinking core model and its application to the direct sulfidation of limestone. *Can J Chem Eng* 71:734–745
17. Efthimiadis EA, Sotirchos SV (1993) Effects of pore structure on the performance of coal gas desulfurization sorbents. *Chem Eng Sci* 48:1971–1984
18. Ulrichson DL, Yake DE (1980) Numerical analysis of a finite cylindrical pellet model in solid-gas reactions. *Chem Eng Sci* 35:2207–2212
19. Zhang Y, Liu BS, Zhang FM, Zhang ZF (2013) Formation of (Fe<sub>x</sub>Mn<sub>2-x</sub>)O<sub>3</sub> solid solution and high sulfur capacity properties of Mn based/M41 sorbents for hot coal gas desulfurization. *J Hazard Mater* 248–249:81–88
20. Doğu T (1981) The importance of pore structure and diffusion in the kinetics of gas–solid non-catalytic reactions: reaction of calcined limestone with SO<sub>2</sub>. *Chem Eng J* 21:213
21. Suyadal Y, Erol M, Oğuz H (2000) Deactivation model for the adsorption of trichloroethylene vapor on an activated carbon bed. *Ind Eng Chem Res* 39:724–730
22. Ozaydin Z, Yasyerli S, Doğu G (2008) Synthesis and activity comparison of copper-incorporated MCM-41-type sorbents prepared by one-pot and impregnation procedures for H<sub>2</sub>S removal. *Ind Eng Chem Res* 47:1035–1042
23. Caglayan P, Yasyerli S, Ar I, Doğu G, Doğu T (2006) Kinetics of H<sub>2</sub>S sorption on manganese oxide and Mn–Fe–Cu mixed oxide prepared by the complexation technique. *Int J Chem React Eng* 4:1–10
24. Yasyerli S (2008) Cerium-manganese mixed oxides for high temperature H<sub>2</sub>S removal and activity comparisons with V–Mn, Zn–Mn, Fe–Mn sorbents. *Chem Eng Process* 47:577–584
25. Dahlan I, Lee KT, Kamaruddin AH, Mohamed AR (2011) Sorption of SO<sub>2</sub> and NO from simulated flue gas over rice husk ash (RHA)/CaO/CeO<sub>2</sub> sorbent: evaluation of deactivation kinetic parameters. *J Hazard Mater* 185:1609–1613
26. Ficicilar B, Doğu T (2006) Breakthrough analysis for CO<sub>2</sub> removal by activated hydrotalcite and soda ash. *Catal Today* 115:274–278
27. Fogler HS (1999) *Elements of chemical reaction engineering*, 3rd edn. Prentice Hall PTR, Upper Saddle River
28. Tang F, Yang XD (2012) A “deactivation” kinetic model for predicting the performance of photocatalytic degradation of indoor toluene, o-xylene, and benzene. *Build Environ* 56:329–334
29. Martín O, Gorka Z, Jose MA, Ana GG, Javier B (1996) Deactivation kinetic model in catalytic polymerizations taking into account the initiation step. *Ind Eng Chem Res* 35:62–69
30. Abbasi E, Arastoopour H (2011) CFD simulation of CO<sub>2</sub> sorption in a circulating fluidized bed using deactivation kinetic model. In: *Proceeding of the 10th conference on circulating fluidized beds and fluidization technology*
31. Ko T (2015) Fitting of breakthrough curve by deactivation kinetic model for adsorption of H<sub>2</sub>S from syngas with Zn-contaminated soil. *Asian J Chem* 27:865–869
32. Hong YS, Zhang ZF, Cai ZP, Zhao XH, Liu BS (2014) Deactivation kinetic model of H<sub>2</sub>S removal over mesoporous LaFeO<sub>3</sub>/MCM-41 sorbent during hot coal gas desulfurization. *Energy Fuels* 28:6012–6018
33. Hong YS, Sin KR, Pak JS, Kim CJ, Liu BS (2017) Kinetic analysis of H<sub>2</sub>S removal over mesoporous Cu–Mn mixed oxide/SBA-15 and La–Mn mixed oxide/KIT-6 sorbents during hot coal gas desulfurization using the deactivation kinetic model. *Energy Fuels* 31:9874–9880


34. Hong YS (2018) Kinetic reevaluation on “Synthesis of a novel nanosilica-supported poly  $\beta$ -cyclodextrin sorbent and its properties for the removal of dyes from aqueous solution.” *Colloids Surf, A* 545:127–129
35. Hong YS (2019) Kinetic re-evaluation on “Comparative adsorption of Pb(II), Cu(II) and Cd(II) on chitosan saturated montmorillonite: kinetic, thermodynamic and equilibrium studies.” *Appl Clay Sci* 175:190–192
36. Sin KR, Hong YS, Kim RC (2021) Evaluation of activation energy on adsorption of tenuazonic acid by inactivated LAB. *J Food Eng* 291:109–110
37. Hong YS, Kim CJ, Sin KR, Pak JS (2018) A new adsorption rate equation in batch system. *Chem Phys Lett* 706:196–201
38. Langmuir I (1918) The adsorption of gases on plane surfaces of glass, mica and platinum. *J Am Chem Soc* 40:1361–1403
39. Gaulke M, Guschin V, Knapp S, Pappert S, Eckl W (2016) A unified kinetic model for adsorption and desorption applied to water on zeolite. *Micro Meso Mater* 233:39–43
40. Bashiri H (2013) A new solution of Langmuir kinetic model for dissociative adsorption on solid surfaces. *Chem Phys Lett* 575:101–106
41. Fan Y, Rajagopalan V, Soares E, Amiridis MD (2001) Use of an unreacted shrinking core model in the reaction of H<sub>2</sub>S with perovskite type sorbents. *Ind Eng Chem Res* 41:4767–4770
42. Garea A, Viguri JR, Irabien A (1997) Kinetics of flue gas desulfurization at low temperatures fly ash/calcium (3/1) sorbent behavior. *Chem Eng Sci* 52:715–732
43. Wouwer AV, Saucez P, Schiesser WE (2004) Simulation of distributed parameter systems using a matlab-based method of lines toolbox: chemical engineering applications. *Ind Eng Chem Res* 43:3469–3477
44. Lagergren SY (1898) Zur theorie der sogenannten adsorption gelöster stoffe kungliga svenska vetenskapsakademiens. *Handlingar* 24:1–39
45. Ho YS, McKay G (1999) Pseudo-second order model for sorption processes. *Process Biochem* 34:451–465
46. Özer A (2007) Removal of Pb(II) ions from aqueous solutions by sulphuric acid-treated wheat bran. *J Hazard Mater* 141:753–761
47. Marczewski AW (2010) Application of mixed order rate equations to adsorption of methylene blue on mesoporous carbons. *Appl Surf Sci* 256:5145–5152
48. Yang X, Al-Duri BJ (2005) Kinetic modeling of liquid-phase adsorption of reactive dyes on activated carbon. *Colloid Interface Sci* 287:25–34
49. Azizian S, Fallah RN (2010) A new empirical rate equation for adsorption kinetics at solid/solution interface. *Appl Surf Sci* 256:5153–5156
50. Haerifar M, Azizian S (2012) Fractal-like adsorption kinetics at solid/solution interface. *J Phys Chem C* 116:13111–13119
51. Haerifar M, Azizian S (2014) Fractal-like kinetics for adsorption on heterogeneous solid surfaces. *J Phys Chem C* 118:1129–1134
52. Haerifar M, Azizian S (2013) An exponential kinetic model for adsorption at solid/solution interface. *Chem Eng J* 215–216:65–71
53. Eris S, Azizian S (2017) Analysis of adsorption kinetics at solid/solution interface using a hyperbolic tangent model. *J Mol Liq* 231:523–527
54. Xiao FZ, Peng GW, Ding DX, Dai YM (2015) Preparation of a novel biosorbent ISCB and its adsorption and desorption properties of uranium ions in aqueous solution. *J Radioanal Nucl Chem* 306:349–356
55. Khawassek YM, Masoud AM, Taha MH, Hussein AEM (2018) Kinetics and thermodynamics of uranium ion adsorption from waste solution using Amberjet 1200 H as cation exchanger. *J Radioanal Nucl Chem* 315:493–502
56. Zhao WH, Lin XY, Cai HM, Mu T, Luo XG (2017) Preparation of mesoporous carbon from sodium lignosulfonate by hydrothermal and template method and its adsorption of Uranium (VI). *Ind Eng Chem Res* 56:12745–12754
57. Abdi S, Nasiri M, Mesbahi A, Khani MH (2017) Investigation of uranium (VI) adsorption by polypyrrole. *J Hazard Mater* 332:132–139
58. Yan TS, Luo XG, Zou ZQ, Lin XY, He Y (2017) Adsorption of Uranium (VI) from a simulated saline solution by alkali-activated leather waste. *Ind Eng Chem Res* 56:3251–3258

59. Yuan DZ, Wang Y, Qian Y, Liu Y, Feng G, Huang B, Zhao XH (2017) Highly selective adsorption of uranium in strong  $\text{HNO}_3$  media achieved on a phosphonic acid functionalized nanoporous polymer. *J Mater Chem A* 5:22735–22742
60. Wan ZY, Liu BS, Zhang FM, Zhao XH (2011) Characterization and performance of  $\text{La}_x\text{Fe}_y\text{O}_z/\text{MCM-41}$  sorbents during hot coal gas desulfurization. *Chem Eng J* 171:594–602
61. Xia H, Zhang FM, Zhang ZF, Liu BS (2015) Synthesis of functional  $x\text{La}_y\text{Mn}/\text{KIT-6}$  and feature of hot coal gas desulfurization. *Phys Chem Chem Phys* 17:20667–20676
62. Truesdale VW (2008) Shrinking sphere kinetics for batch dissolution of mixed particles of a single substance at high under-saturation: validation with sodium chloride. *Aquat Geochem* 14:359–379
63. Cai J, Liu L, Li Z (2021) Rate equation theory for the hydrogenation kinetics of Mg-based materials. *Int J Hydrogen Energy* 46:30061–30078
64. Zhang X, Zhu Z, Wen G, Lang L, Wang M (2021) Study on gas desorption and diffusion kinetic behavior in coal matrix using a modified shrinking core model. *J Pet Sci Eng* 204:108701
65. Arunachalam T, Karpagasundaram M, Rajarathinam N (2018) Adsorption of acid yellow 36 onto green nanoceria and amine functionalized green nanoceria: comparative studies on kinetics, isotherm, thermodynamics, and diffusion analysis. *J Taiwan Inst Chem Eng* 93:211–225
66. Bettoni M, Falcinelli S, Rol C, Rosi C, Sebastiani M (2021) Gas-phase  $\text{TiO}_2$  photosensitized mineralization of some VOCs: mechanistic suggestions through a Langmuir–Hinshelwood kinetic approach. *Catalysts* 11(20):1–14
67. Andrieux J, Demirci UB, Miele P (2011) Langmuir–Hinshelwood kinetic model to capture the cobalt nanoparticles-catalyzed hydrolysis of sodium borohydride over a wide temperature range. *Catal Today* 170:13–19

**Publisher's Note** Springer Nature remains neutral with regard to jurisdictional claims in published maps and institutional affiliations.

Springer Nature or its licensor (e.g. a society or other partner) holds exclusive rights to this article under a publishing agreement with the author(s) or other rightsholder(s); author self-archiving of the accepted manuscript version of this article is solely governed by the terms of such publishing agreement and applicable law.

## Authors and Affiliations

Kye-Ryong Sin<sup>1</sup>  · Yong-Son Hong<sup>2</sup> · Ju-Gyong Kim<sup>1</sup> · Wi-Ryong Choe<sup>2</sup> · Kwang-Song Kim<sup>2</sup> · Yong-Man Jang<sup>1</sup>

✉ Kye-Ryong Sin  
gr.sin@ryongnamsan.edu.kp

<sup>1</sup> Faculty of Chemistry, Kim Il Sung University, Taesong District, Pyongyang, Democratic People's Republic of Korea

<sup>2</sup> Faculty of Chemistry, Kim Hyong Jik University of Education, Tongdaewon District, Pyongyang, Democratic People's Republic of Korea